bioRxiv preprint doi: https://doi.org/10.1101/2020.09.08.287888. this version posted September 9, 2020. The copyright holder for this preprint (which was not certified by peer review) is the author/funder. It is made available under a CC-BY 4.0 International license.

Heteroscedastic regression modeling elucidates gene-by-environment interaction

Benjamin W. Domingue[1,2,†], Klint Kanopka[1], Travis T. Mallard[3], Sam Trejo[4,5], and Elliot M. Tucker-Drob[3,6,†]

[1]Graduate School of Education, Stanford University
[2]Center for Population Health Sciences, Stanford Medicine
[3]Department of Psychology, University of Texas at Austin
[4]La Follette School of Public Affairs, University of Wisconsin–Madison
[5]Department of Sociology, University of Wisconsin–Madison
[6]Population Research Center, University of Texas at Austin
[†]bdomingu@stanford.edu; tuckerdrob@utexas.edu

Abstract

Genotype-by-environment interaction (GxE) occurs when the size of a genetic effect varies systematically across levels of the environment and when the size of an environmental effect varies systematically across levels of the genotype. However, total variance in the phenotype may shift as a function of the moderator irrespective of its etiology such that the *proportional* effect of the predictor is constant. We expand the traditional GxE regression model for polygenic scores and single locus allele counts to directly account for heteroscedasticity associated with both the genotype and the measured environment, and we derive a test statistic, ξ, for inferring whether GxE can be plausibly attributed to a more general effect of the genetic or environmental moderator on the dispersion of the phenotype. We apply this method to test whether genotype-by-birth year interactions for Body Mass Index (BMI) are distinguishable from general secular increases in the variance of BMI or associations of the genetic predictors (both PGS and individual loci) with BMI variance. We provide software for estimating heteroscedastic GxE regression models and calculating ξ.

Key Words: gene-by-environment interaction, gene × environment interaction, GxE, G×E, vQTL, heteroscedasticity.

1 Introduction

Genotype-by-Environment interaction (GxE) studies test whether the genotype-phenotype association varies in magnitude across the range of a measured environmental variable and whether the environment-phenotype association varies in magnitude across the range of the measured genotype. Investigations of GxE have been of particular interest in the study of complex traits, leading to a variety of methods for estimating polygenic GxE [1, 2]. Development of these analytic approaches coincides with a large increase in the availability of genomic data, particularly in the context of population-based studies that also contain a broad range of phenotypes and environmental measures. Here, we consider circumstances where either the genetic or the environmental measure selected for GxE is associated with the magnitude of variance in the target phenotype. Such heteroscedasticity introduces a key interpretational problem to results from standard GxE approaches: any observed GxE may arise as an artifact of the fact that the total variance in the phenotype shifts across the range of the genetic or environmental moderator, irrespective of etiology. We resolve this problem by expanding the standard regression-based model for testing GxE in both single locus and polygenic score settings by introducing a simple yet flexible approach to directly

bioRxiv preprint doi: https://doi.org/10.1101/2020.09.08.287888. this version posted September 9, 2020. The copyright holder for this preprint (which was not certified by peer review) is the author/funder. It is made available under a CC-BY 4.0 International license.

model heteroscedastic residuals, and we develop a test statistic for inferring whether GxE can be plausibly attributed to a more general effect of the moderator on the dispersion of the phenotype.

All else equal, when the dispersion of a phenotype is directly controlled by the level of the moderator, the standard regression-based model will identify a significant interaction between that moderator and *any* correlate of the phenotype, whether genetic or non-genetic. For example, when the effectiveness, intensity, or dosage of a phenotype-altering intervention varies proportionally to baseline levels of the phenotype (e.g. when hours of individualized education are assigned based on previous year's test scores; or when intensity of a weight-loss intervention is determined from baseline body mass index), then the variance of the phenotype is expected to increase in response to the intervention, and the unstandardized effect sizes for all correlates of baseline levels of the phenotype are expected to increase. Similarly, when a genetic variant confers greater plasticity in a phenotype, then the variance of the phenotype is expected to differ across alleles (such that the variant is identified as a variance quantitative trait locus, vQTL). We would then expect the variant to moderate the effect sizes for all correlates of that phenotype proportionally to one another. Only when a moderator acts preferentially on specific mechanisms of variation in the phenotype are interactions with various predictors expected to depart from expectations that follow from differences in total variance across the range of the moderator.

Figure 1 illustrates how heteroscedasticity across the range of a measured environmental moderator (E; left panel) or genetic moderator (G; right panel) can produce the impression of GxE. In the left panel, we illustrate a scenario in which a PGS is associated with a constant proportion of variance in the phenotype across the range of the measured environment. That the proportion of variance explained by the PGS at any given location on the x-axis is constant indicates that the expected percentile location within the distribution of the phenotype will also be constant across the range of E (assuming that the shape, but not dispersion, of the distribution remains constant across the range of E). Nevertheless, a clear fan-spreading effect is observed, incorrectly implying that the PGS is increasingly penetrant at higher levels of E. The right panel represents an analogous scenario with respect to a single genetic variant that moderates the variance of the phenotype (i.e a vQTL [3, 4, 5, 6, 7]). In this scenario, the environment is associated with a constant proportion of variance in the phenotype across the range of the genotype, but appears to become increasingly predictive of the phenotype as the effect allele count increases as a result of heteroscedasticity. By directly modeling this heteroscedasticity, we are able to distinguish between scenarios such as these—in which GxE is an epiphenomenon of variance modulation—from those representing more meaningful patterns of GxE.

We develop and validate a flexible heteroscedastic regression model for testing GxE. We apply this model elucidate to the well-studied interaction between birth cohort and genetics linked to body mass index (BMI). We test whether both PGS-by-Birth Year and SNP-by-Birth Year interactions on BMI can be attributed to more general increases in the total dispersion of BMI over historical time. That is, we ask whether birth year is associated specifically with amplification of genetic risk for BMI or more generally with amplification of all variation in BMI.

2 Results

2.1 Overview of Method

In settings wherein focus is on a measured genotype, as indexed by a single-locus allele count or a polygenic score (PGS), the standard regression model for GxE is

$$Y_i = \beta_0 + \beta_1 G_i + \beta_2 E_i + \beta_3 G_i \cdot E_i + e_i, \tag{1}$$

where Y_i is the phenotype for person i, G_i is the measured genotype, E_i is the measured environment, and e_i is an error term. Under this model, the effect of G_i on Y_i is allowed to vary as a linear function of E_i, as indexed by the regression coefficient β_3. However, a crucial assumption is that the residuals, e_i, are homoscedastic across all levels of E_i (e.g., $e_i \sim \mathrm{N}(0, \sigma^2_\epsilon)$).

The standard regression model given by Eqn 1 can be expanded so as to relax the assumption of homoscedasticity of residuals across E_i by specifying the following *environmental heteroscedasticity*

bioRxiv preprint doi: https://doi.org/10.1101/2020.09.08.287888. this version posted September 9, 2020. The copyright holder for this preprint (which was not certified by peer review) is the author/funder. It is made available under a CC-BY 4.0 International license.

Figure 1: Hypothetical examples of an Environmental moderator (left) or a genetic moderator (right) of total variance in a phenotype producing the impression of GxE. Left: Residuals of the regression of the Phenotype on the Measured Environment are heteroscedastic. high, average, and low polygenic scores (PGSs) are associated with constant percentiles of the phenotype at any given location along the x axis. However, because variance of the phenotype expands across the range of the Measured Environment, the PGS accounts for increasing unstandardized variance across this range. Right: A variance quantitative trait locus (vQTL) in which the effect allele is associated with greater variance in the phenotype. Unstandardized scores on the phenotype that are associated with high, average, and low levels of the measured environment (E) become more distinct with increasing number of effect alleles. However, because the total variance in the phenotype expands across the x axis, the *percentile* locations of these scores within each genotype (0, 1, or 2) is constant across all levels of the genotype.

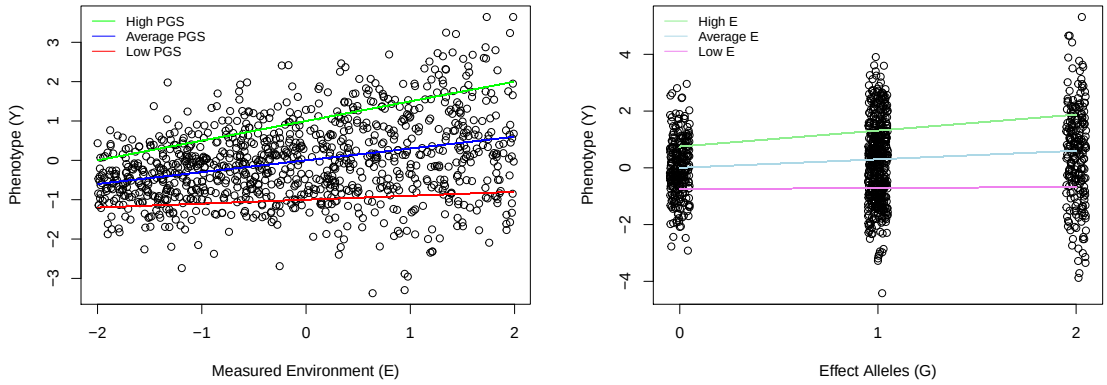

model,

$$Y_i = \tau_0 + \tau_1 E_i + \pi_0 G_i + \pi_1 G_i \cdot E_i + \lambda_0 \epsilon_i + \lambda_1 E_i \cdot \epsilon_i. \quad (2)$$

Here, τ_1 is the main effect of the measured environment, π_0 is the main effect of G_i, π_1 is the GxE analogue to β_3 in Eqn 1, λ_0 is the main effect of the error ϵ_i (which we assume, without loss of generality given λ_0, to have unit variance), and λ_1 is the coefficient used to index heteroscedasticity. Note that the heteroscedasticity term $E_i \cdot \epsilon_i$ takes a form parallel to the GxE term, $G_i \cdot E_i$.

The heteroscedasticity model is a flexible model allowing for both conventional GxE and heteroscedasticity. In order to test whether a more general pattern of heteroscedasticity as a function of E_i is sufficient to account for the observed GxE, we propose a restricted form version of this model that does not directly model GxE but instead allows for the total variance of the phenotype to vary as a function of E_i. This *scaling model* represents a scenario wherein GxE—in the sense of a significant estimate of β_3 in Eqn 1—arises as a function of differences in the total variance of Y_i as a function of E_i. We choose this nomenclature given that the model emphasizes the importance of the *scale* of the outcome. Under this model, the proportional contribution of G_i is constant over the range of E_i, but the scale of Y_i systematically varies across the range of E_i; i.e., E_i acts as a "dimmer" [8].

The scaling model for moderation of the variance of Y_i as a function of E_i takes the form

$$Y_i = a_0 + a_1 E_i + (b_0 + b_1 E_i) Y_i^\star. \quad (3)$$

Here, $Y_i^\star$ is an unobserved factor representing unexplained variation in Y_i incremental of E_i. The $b_0 + b_1 E_i$ coefficient on the $Y^\star$ term produces heteroscedasticity in Y_i as a function of E_i. We let

$$Y_i^\star = hG_i + e\epsilon_i \quad (4)$$

where G is a measured genotype standardized to have unit variance and ϵ_i is an unobserved error term (we assume it is also scaled to have unit variance). Finally, we identify the units of $Y^\star$

bioRxiv preprint doi: https://doi.org/10.1101/2020.09.08.287888. this version posted September 9, 2020. The copyright holder for this preprint (which was not certified by peer review) is the author/funder. It is made available under a CC-BY 4.0 International license.

by specifying $e = \sqrt{1-h^2}$. The penetrance of the measured genotype is thus controlled via the relative magnitudes of h and e. Note, in particular, that in terms of $Y_i^\star$, the penetrance of the measured genotype is constant. The test that we introduce relies on this property; i.e., when properly scaled, the penetrance of the measured genotype to Y_i is constant. Suppose that $b_1 = 0$. In that case, Y_i is affected solely by environmental and genetic main effects. If $b_1 \neq 0$, then the role of $Y_i^\star$ with respect to Y_i varies as a function of E, and as we elucidate next, so do the raw (but not relative) contributions of G_i and ϵ_i to Y.

In Section A of the supplemental information (SI), we show that the environmental heteroscedasticity model reduces to the environmental scaling model when

$$\frac{\pi_0}{\lambda_0} = \frac{\pi_1}{\lambda_1}. \tag{5}$$

We use this observation to derive the test statistic ξ_E and associated hypothesis test of whether an empirical estimate of GxE is distinguishable from the scaling model as

$$\xi_E \equiv \widehat{\pi_0}\widehat{\lambda_1} - \widehat{\pi_1}\widehat{\lambda_0}, \tag{6}$$

$$H_0 : \xi_E = 0. \tag{7}$$

We provide parallel heteroscedasticity and scaling models for moderation of the variance of Y_i as a function of G_i (leading to an analogous test statistic, ξ_G) in Section A.3 of SI.

We conduct a variety of simulation studies (see Section B of SI). In summary, results of the simulation study suggest that ξ_E is a reliable indicator of whether the scaling model is the basis for GxE. When a test of the statistic fails to reject $H_0 : \xi_E = 0$ and there is significant GxE (π_1) observed, we cannot rule out that the scaling model is driving observed GxE. When the test suggests rejection of $H_0 : \xi_E = 0$, alternative forms of GxE are implicated. Software to estimate the models considered here is described in Section C of SI.

2.2 Heteroscedasticity in context of BMI-linked genetics and birth year

We apply our heteroscedastic GxE model to the well-studied interaction between birth year and genetics linked to body mass index (BMI) [9, 10, 11, 12].[1] We test whether previous reports of increasing penetrance of PGS for BMI for later-born birth cohorts can be plausibly attributed to more general increases in the total dispersion of BMI, including variation unique of its genetic etiology, across birth cohorts [14, 15]. We thus ask whether birth year is associated specifically with amplification of genetic risk for BMI or more more generally with amplification of all variation in BMI. We then go on to apply our heteroscedastic GxE model to examine individual locus-by-year interactions for BMI. To illustrate how our approach can be used to conduct SNP-level analyses, we apply our technique using the top hits from a recent BMI GWAS [16] to investigate whether they are associated with heteroscedastic GxE.

2.2.1 Polygenic Score Analysis

We consider GxE in the context of a long-running cohort study—the Health and Retirement Study (HRS) [17]—of US adults over 50 and their spouses (N=11,586). Respondents are interviewed every two years and data are collected on their early-life, anthropometrics, socioeconomic status, and mental and physical well-being. Previous examinations of increases in the penetrance of the BMI polygenic score across birth year have used this data [9, 10, 11]. We use a polygenic score for BMI [16] as constructed by the HRS [18]; further description of the data are in D of SI.

Results are presented in Table 1. We first analyze all respondents together and then conduct separate analyses by sex. In all cases, we observe considerable evidence for stronger prediction of BMI by the PGS for more recently born individuals (i.e., $\pi_1 > 0$); this is consistent with earlier findings indicating secular increases in the penetrance of a BMI PGS [9, 10, 11]. However, we also observe considerable evidence for non-PGS variance in BMI to increase with birth year (i.e.,

[1] A literal textbook example, see Section 11.3 of [13].

bioRxiv preprint doi: https://doi.org/10.1101/2020.09.08.287888. this version posted September 9, 2020. The copyright holder for this preprint (which was not certified by peer review) is the author/funder. It is made available under a CC-BY 4.0 International license.

$\lambda_1 > 0$), raising the possibility that the obtained GxE may be attributable to a more general pattern of increasing variance in BMI with birth year. In sex-pooled analyses, probabilities associated with tests of H_0 are ≈ 0.02. However, findings vary slightly by gender; especially for males, we are unable to reject the null of the scaling model.

Table 1: Estimates from parameters of the full heteroscedasticity model (Eqn 42) in analysis of GxE for BMI as a function of birth year in the HRS. The ξ_E and ξ_G estimates reported are obtained from the environmental and genetic heteroscedasticity models, respectively. We show probabilities for parameters when the maximal probability in a column is larger than $1e-6$.

Gender	BMI[a]	N	τ_1	π_0	π_1	$\Pr_{\pi_1}$	λ_0	λ_1	λ_2	$\Pr_{\lambda_2}$	$\Pr_{\xi_E}$	$\Pr_{\xi_G}$
All	Std	11586	0.19	0.25	0.06	1.78e-11	0.93	0.12	0.09	7.44e-50	1.76e-02	7.89e-04
All	Trans	11586	0.17	0.26	0.04	1.79e-05	0.95	0.06	0.02	1.14e-03	2.68e-02	5.15e-04
M	Std	5022	0.19	0.26	0.04	4.69e-04	0.93	0.12	0.09	1.63e-22	3.91e-01	2.75e-01
M	Trans	5022	0.17	0.26	0.03	2.11e-02	0.95	0.07	0.03	1.33e-03	3.83e-01	1.65e-01
F	Std	6564	0.20	0.25	0.06	6.65e-09	0.93	0.12	0.09	3.52e-31	2.24e-02	1.21e-03
F	Trans	6564	0.18	0.26	0.04	2.08e-04	0.94	0.06	0.02	1.11e-02	3.82e-02	1.75e-03

[a] Std denotes the standardized mean BMI shown in the middle panel of Figure D.1. Trans denotes the Box-Cox transformation.

To better illustrate the differences in the sex-stratified analyses, we consider a graphical analysis inspired by the notion of posterior predictive checks [19]. Using estimates from the empirical data, we construct simulated data sets using Eqn 14 and Eqn 1 and the HRS data. We then consider the predicted percentage of phenotypic variance explained by the genetic predictor across birthyears. Based on Eqn 9, we compute this percentage as

$$\frac{Vg}{Vp} = \frac{(\pi_0 + \pi_1 E)^2}{(\pi_0 + \pi_1 E)^2 + (\lambda_0 + \lambda_1 E)^2}. \tag{8}$$

Results of this graphical analysis are in Figure 2. For males (top row), the empirical data (in red) produce a pattern that falls well within the distribution of results from data simulated from the scaling model, but departs more appreciably from results from data simulated under the conventional homoscedastic GxE model. The proportional contribution of the PGS to BMI does not significantly increase with birth year for males. For females, there is more change in penetrance than would be anticipated under the scaling model but less change than would be anticipated under the conventional homoscedastic GxE model. As compared to males,the proportional contribution of the PGS to BMI significantly increases with birth year for females. Thus, for females, the full heteroscedasticity model, in which the contributions of PGS and non-PGS factors independently shift with birth year, may be the most appropriate analytic tool.

We also illustrate the potential for genetic heteroscedasticity using the genetic heteroscedasticity model (Eqn 37). We observe evidence for moderation of residual variance in BMI by the BMI PGS, as indicated by the λ_2 parameter. Interestingly, this result holds even for the Box-Cox transformed version of BMI, suggesting that the heteroscedasticity is not entirely an artifact of mean-variance associations induced by the skewed distribution of BMI. One interpretation of these results is that the polygenic score for BMI also captures some degree of "plasticity" (in the sense of [20]). Results of the ξ_G tests (see final column of Table 1) are similar to those of the ξ_E in that we cannot reject the null of the scaling model for the male respondents.

2.2.2 SNP Analyses

We conducted heteroscedastic regression analyses for 96 marker SNPs for the genome-wide significant loci identified in [16] using independent data from N=380,605 participants from UK Biobank (UKB; not used in the [16] GWAS). Replication results for the main effects can be found in Table F.2. Note that the UKB is highly non-representative [21] potentially affecting the generalizability of our results.

The environmental heteroscedasticity parameter (λ_1) was positive and significant in all models, suggesting greater variance in BMI among those born later in the 20th century. With the full heteroscedasticity model, we identified four SNPs that exhibited significant gene-by-birth year effects,

bioRxiv preprint doi: https://doi.org/10.1101/2020.09.08.287888. this version posted September 9, 2020. The copyright holder for this preprint (which was not certified by peer review) is the author/funder. It is made available under a CC-BY 4.0 International license.

Figure 2: Gray lines represent genetic penetrance as a function of birth year simulated based on either the scaling model (Eqn 14, on left) or the standard homoscedastic GxE model (Eqn 1, on right). Red lines represent genetic penetrance as a function of birth year estimated from the real data using the heteroscedastic regression model (Eqn 9). Analyses based on standardized BMI data.

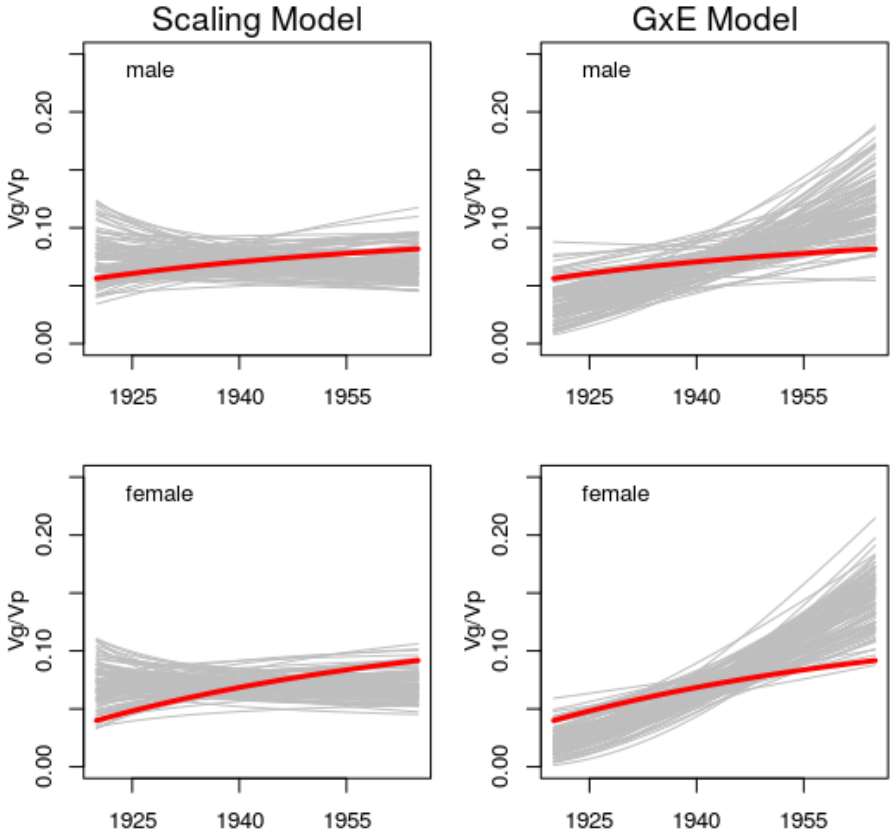

as indicated by the π_1 parameter at the Bonferroni-adjusted alpha level. Parameter estimates from the full heteroscedasticity model for these SNPs are reported in Table 2, along with ξ_E and ξ_G estimates obtained from the environmental and genetic heteroscedasticity models, respectively. Note that rs1558902 is a variant in the FTO gene locus. This finding replicates earlier results [22] which reported increasing penetrance of a variant with FTO over historical time using a different data set. However, ξ_G was highly significant for each of these four SNPs, allowing us to reject the null that observed GxE is driven entirely by scaling.

With the full heteroscedasticity model, we identified six SNPs that exhibited significant effects on the dispersion of BMI, as indicated by the λ_2 parameter at the Bonferroni adjusted alpha level. Parameter estimates for these SNPs are reported in the supplement (Table F.1), along with ξ_E and ξ_G estimates obtained from the environmental and genetic heteroscedasticity models, respectively. Of the 4 Bonferonni significant variants for SNP-by-Year interaction described above, only the FTO variant (rs1558902) appears among the 6 Bonferonni significant variants for vQTL. This finding replicates earlier results [3] reporting that the FTO gene locus is associated with greater variability in BMI. The p value of ξ_G for this variant is 5.1e-07, indicating the the above-reported SNP-by-birth-year interaction on BMI for FTO is not simply attributable to a general modulation of variance by rs1558902. Note that although the ξ_G statistic is not significant for rs7903146, rs9925964, and rs2287019, these SNPs do not exhibit GxE at Bonferonni-corrected levels, rendering the ξ_G moot.

To examine the total evidence of signal for GxE and genetic heteroscedasticity in the 96 SNPs,

bioRxiv preprint doi: https://doi.org/10.1101/2020.09.08.287888. this version posted September 9, 2020. The copyright holder for this preprint (which was not certified by peer review) is the author/funder. It is made available under a CC-BY 4.0 International license.

we provide a QQ plot of -1og10(p) for parameters indexing SNP-controlled heteroscedasticity of BMI vQTL and gene-by-birth year GxE interaction for Box-Cox transformed BMI in the left panel of Figure 3. We observe considerable departure of the observed -1og10(p) values relative to the expectation under the null, indicating strong enrichment of signal for both vQTL and GxE. In the right panel of Figure 3, we provide the scatter plots of parameter estimates for SNP main effects ($\pi 0$), GxE (π_1), for vQTL (λ_2) for Box-Cox transformed BMI. We observe moderate-to-strong associations between the main effect of a SNP and both its GxE and vQTL effects, indicating that, among these variants selected on the basis of marking genome-wide significant loci for BMI in an external meta-analysis, those with larger main effects on BMI exhibit larger interactions with birth year and more pronounced moderation of BMI variance. Results of [6] suggest that similar patterns may apply genome-wide.

Our results indicate that SNP moderation of birth year effects on BMI and SNP moderation of BMI dispersion were in the same direction as the SNP effects on BMI means. We observe considerable sign congruence between SNP main effects (π_0) and SNP-by-Birth-Year interaction (π_0) for 3 out of 4 SNPs exhibiting Bonferonni significant π_1 estimates and for 71 out of 96 of all SNPs tested. We also observe considerable sign congruence between SNP main effects (π_0) and vQTL effects (λ_2) for 6 out of 6 SNPs exhibiting Bonferonni significant λ_2 estimates, and for 75 out of 96 of all SNPs tested.

Finally, we note that the main effect of birth year (τ_1) was approximately -0.058 in all models (all associated probabilities less than 1e-250), indicating that later-born UK Biobank participants tend to have lower BMI. Given substantial epidemiological evidence from representative samples indicating increasing BMI with birth year, we speculate that this negative association may be driven by selection bias in the UKB sample [21]. However, note that, despite decreasing mean BMI with birth year in this sample, we observe increasing variance in BMI with birth year (as indicated by the positive λ_1 parameter), and increasing penetrance of SNPs with birth year (as indicated by strong sign congruence between π_0 and π_1 parameters). This further suggests that variance moderation and SNP-by-Birth Year interactions are unlikely to have resulted from positive associations between BMI mean and variance.

Table 2: Estimates from parameters of the full heteroscedasticity model (Eqn 42) in analysis of GxE for Box-Cox transformed BMI as a function of birthyear in the UK Biobank for those SNPs with significant π_1 estimates following Bonferonni adjustment. The ξ_E and ξ_G estimates reported are obtained from the environmental and genetic heteroscedasticity models, respectively. We show probabilities for parameters when the maximal probability in a column is larger than $1e-6$.

SNP	π_0	π_1	$\Pr_{\pi_1}$	λ_0	λ_1	λ_2	$\Pr_{\lambda_2}$	$\Pr_{\xi_E}$	$\Pr_{\xi_G}$
rs543874_A	-0.0271	-0.0085	1.90e-07	0.9873	0.0369	-0.0036	1.48e-03	4.39e-06	1.04e-07
rs13021737_G	0.0279	0.0062	1.33e-04	0.9873	0.0369	0.0036	1.53e-03	1.46e-03	1.75e-04
rs1558902_T	-0.0503	-0.0077	2.12e-06	0.9864	0.0368	-0.0096	1.76e-17	2.96e-04	5.14e-07
rs2075650_A	0.0113	-0.0060	2.43e-04	0.9875	0.0371	-0.0002	8.53e-01	2.01e-04	5.78e-04

3 Discussion

When GxE is detected using the conventional regression-based model, it is common to interpret the interaction in terms of the specific genetic and environmental measures included in the interaction model. However, GxE may arise more generally when the genetic or environmental predictor moderates the total amount of variation in the phenotype. When the total amount of variation in a phenotype varies across the range of an environmental measure, traditional homoscedastic GxE models will detect interactions between that measure and all other correlates of the phenotype, both genetic and non-genetic. Here, we have delineated an expanded *heteroscedastic* GxE regression model that explicitly allows for heteroscedasticity in the phenotype as a function of the genetic and environmental measures. We use this model to derive a test statistic, ξ, which compares this

bioRxiv preprint doi: https://doi.org/10.1101/2020.09.08.287888. this version posted September 9, 2020. The copyright holder for this preprint (which was not certified by peer review) is the author/funder. It is made available under a CC-BY 4.0 International license.

Figure 3: Left: QQ plot of -1og10(p) for parameters indexing SNP-by-birth year interaction (GxE, as indicated by the π_1 parameter) and SNP-controlled heteroscedasticity of BMI (vQTL, as indicated by the λ_2 parameter) for Box-Cox transformed BMI. The considerable departure of the observed -1og10(p) values relative to the expectation under the null indicates strong enrichment of signal for both vQTL and GxE in these 96 SNPs previously associated with mean BMI in independent data [16]. Right: Multipanel Scatterplot of the parameters for the SNP main effect (π_0), SNP-by-Birth Year interaction (π_1), and vQTL (λ_2) for Box-Cox transformed BMI. We analyzed 96 marker SNPs for the genome-wide significant loci for BMI identified in [16] in independent data

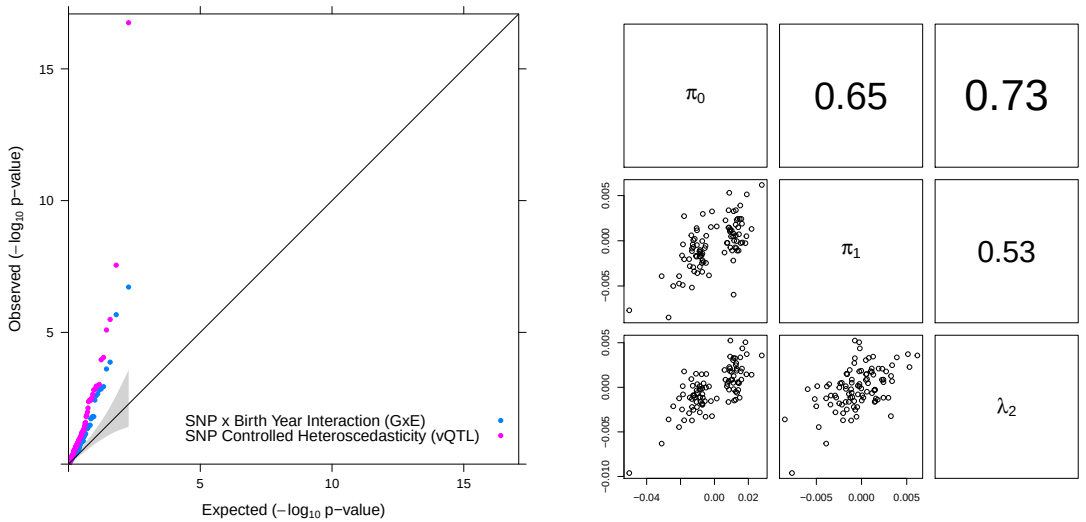

heteroscedasticity model to a simpler *scaling model* in which GxE arises from more general differences in phenotypic variance, irrespective of etiology. When the scaling model holds, differences in phenotypic variance across the range of the genetic or environmental moderator induce a form of GxE that is only apparent in unstandardized units; the proportional contribution of the remaining predictors to phenotypic variance remains constant across the range of the moderator.

We provide an application of the heteroscedastic regression model to empirical data, replicating previous observations that that genetic predictors of BMI have become increasingly penetrant in recent years. However, we additionally observed that the total variance in BMI, including variation not associated with the genetic predictors, increased with participant birthyear. We found that, amongst males within the sample, the interaction between PGS and birth year was indistinguishable from a scaling model in which the total variance in BMI increases over birth year. For males, although the unstandardized variance in BMI accounted for by the PGS increased with birth year, the variance in BMI unaccounted for by the PGS also increased, such that the proportion of variance accounted for in BMI did not significantly vary with birth year. Other work has considered the potential moderation of genetic risk for BMI as a function of diet [23, 24], other lifestyle characteristics [25], and educational attainment [26]. The issues discussed here may be a relevant feature of such empirical work; i.e., environmentally-linked heteroscedasticity may play a role in driving previously observed GxE findings.

We have considered situations in which the dispersion of the phenotype systematically varies as a function of the genetic and environmental measures included in the model. However, other issues surrounding the scaling of the phenotype also have the potential to have substantive effects on GxE results. For instance, skew in the distribution of the phenotype may produce both GxE and heteroscedasticity that would vanish under a transformation. This issue has been vexed geneticists since the days of Fischer [27], and is yet to be fully resolved. In our empirical analysis of BMI, we report results of GxE analyses for both the original scale and a normalizing (Box-Cox) transform of BMI and obtain similar results. In situations in which the phenotype is measured by self-reported

bioRxiv preprint doi: https://doi.org/10.1101/2020.09.08.287888. this version posted September 9, 2020. The copyright holder for this preprint (which was not certified by peer review) is the author/funder. It is made available under a CC-BY 4.0 International license.

items, as is often the case in large-scale epidemiological research, psychometric issues may magnify this problem.

The methods introduced here can be viewed as complementary to those based in other genetic research designs, such as twin/family [1] and genome-wide molecular methods [2] that focus on GxE in the form of differences in the magnitude of of genetic variance or (SNP) heritability across the environmental range. The techniques developed here could be incorporated along with other recently developed GxE techniques [28], as well as techniques to further relax assumptions regarding the parametric form of the likelihood [29, 30], to further enhance the robustness of future GxE work.

GxE research faces a number of conceptual and statistical challenges [8]. Thoughtfully and rigorously engaging with these challenges is particularly salient given the substantial recent increases in the availability of both genetic resources [31] and computational tools [32] for such research. Our proposed test is designed to help clarify the nature of potential GxE findings and to shed additional light on the processes contributing to variation in the phenotype; in particular, we can assess the extent to which the genetic etiology is relatively stable across the range of the environmental measure. Using the model and test statistic presented here, researchers can test for whether variance in the phenotype that is not explained by the genetic predictor shifts across the range of the environment and whether a scaling model may account for the obtained pattern of GxE. When the scaling model holds, we would suggest that the environment largely acts as a "dimming" mechanism on phenotypic variation [8] without altering the proportional contribution of genetic variation to the phenotype.

References

[1] Shaun Purcell. Variance components models for gene–environment interaction in twin analysis. *Twin Research and Human Genetics*, 5(6):554–571, 2002.

[2] Guiyan Ni, Julius van der Werf, Xuan Zhou, Elina Hyppönen, Naomi R Wray, and S Hong Lee. Genotype–covariate correlation and interaction disentangled by a whole-genome multivariate reaction norm model. *Nature communications*, 10(1):1–15, 2019.

[3] Jian Yang, Ruth JF Loos, Joseph E Powell, Sarah E Medland, Elizabeth K Speliotes, Daniel I Chasman, Lynda M Rose, Gudmar Thorleifsson, Valgerdur Steinthorsdottir, Reedik Mägi, et al. Fto genotype is associated with phenotypic variability of body mass index. *Nature*, 490(7419):267–272, 2012.

[4] Huanwei Wang, Futao Zhang, Jian Zeng, Yang Wu, Kathryn E Kemper, Angli Xue, Min Zhang, Joseph E Powell, Michael E Goddard, Naomi R Wray, et al. Genotype-by-environment interactions inferred from genetic effects on phenotypic variability in the uk biobank. *Science advances*, 5(8):eaaw3538, 2019.

[5] Dalton Conley, Rebecca Johnson, Ben Domingue, Christopher Dawes, Jason Boardman, and Mark Siegal. A sibling method for identifying vqtls. *PloS one*, 13(4):e0194541, 2018.

[6] Alexander I Young, Fabian L Wauthier, and Peter Donnelly. Identifying loci affecting trait variability and detecting interactions in genome-wide association studies. *Nature genetics*, 50(11):1608–1614, 2018.

[7] Andrew R Marderstein, Emily Davenport, Scott Kulm, Cristopher V Van Hout, Olivier Elemento, and Andrew G Clark. Leveraging phenotypic variability to identify genetic interactions in human phenotypes. *bioRxiv*, 2020.

[8] Benjamin Domingue, Sam Trejo, Emma Armstrong-Carter, and Elliot M Tucker-Drob. Interactions between polygenic scores and environments: Methodological and conceptual challenges. *Sociological Science*, In press.

bioRxiv preprint doi: https://doi.org/10.1101/2020.09.08.287888. this version posted September 9, 2020. The copyright holder for this preprint (which was not certified by peer review) is the author/funder. It is made available under a CC-BY 4.0 International license.

[9] Dalton Conley, Thomas M Laidley, Jason D Boardman, and Benjamin W Domingue. Changing polygenic penetrance on phenotypes in the 20 th century among adults in the us population. *Scientific reports*, 6:30348, 2016.

[10] Hexuan Liu and Guang Guo. Lifetime socioeconomic status, historical context, and genetic inheritance in shaping body mass in middle and late adulthood. *American sociological review*, 80(4):705–737, 2015.

[11] Stefan Walter, Iván Mejía-Guevara, Karol Estrada, Sze Y Liu, and M Maria Glymour. Association of a genetic risk score with body mass index across different birth cohorts. *Jama*, 316(1):63–69, 2016.

[12] Ellen W Demerath, Audrey C Choh, William Johnson, Joanne E Curran, Miryoung Lee, Claire Bellis, Thomas D Dyer, Stefan A Czerwinski, John Blangero, and Bradford Towne. The positive association of obesity variants with adulthood adiposity strengthens over an 80-year period: a gene-by-birth year interaction. *Human heredity*, 75(2-4):175–185, 2013.

[13] Melinda C Mills, Nicola Barban, and Felix C Tropf. *An Introduction to Statistical Genetic Data Analysis*. MIT Press, 2020.

[14] Katherine M Flegal, Deanna Kruszon-Moran, Margaret D Carroll, Cheryl D Fryar, and Cynthia L Ogden. Trends in obesity among adults in the united states, 2005 to 2014. *Jama*, 315(21):2284–2291, 2016.

[15] Cynthia L Ogden, Cheryl D Fryar, Crescent B Martin, David S Freedman, Margaret D Carroll, Qiuping Gu, and Craig M Hales. Trends in obesity prevalence by race and hispanic origin—1999-2000 to 2017-2018. *JAMA*.

[16] Adam E Locke, Bratati Kahali, Sonja I Berndt, Anne E Justice, Tune H Pers, Felix R Day, Corey Powell, Sailaja Vedantam, Martin L Buchkovich, Jian Yang, et al. Genetic studies of body mass index yield new insights for obesity biology. *Nature*, 518(7538):197–206, 2015.

[17] F Thomas Juster and Richard Suzman. An overview of the health and retirement study. *Journal of Human Resources*, pages S7–S56, 1995.

[18] Erin Ware, Lauren Schmitz, Arianna Gard, and Jessica Faul. Hrs polygenic scores—release 3: 2006–2012 genetic data. *Ann Arbor: Survey Research Center, University of Michigan*, 2018.

[19] Andrew Gelman, Xiao-Li Meng, and Hal Stern. Posterior predictive assessment of model fitness via realized discrepancies. *Statistica sinica*, pages 733–760, 1996.

[20] Rebecca Johnson, Ramina Sotoudeh, and Dalton Conley. Polygenic scores for plasticity: A new tool for studying gene-environment interplay. *bioRxiv*.

[21] Anna Fry, Thomas J Littlejohns, Cathie Sudlow, Nicola Doherty, Ligia Adamska, Tim Sprosen, Rory Collins, and Naomi E Allen. Comparison of sociodemographic and health-related characteristics of uk biobank participants with those of the general population. *American journal of epidemiology*, 186(9):1026–1034, 2017.

[22] James Niels Rosenquist, Steven F Lehrer, A James O'Malley, Alan M Zaslavsky, Jordan W Smoller, and Nicholas A Christakis. Cohort of birth modifies the association between fto genotype and bmi. *Proceedings of the National Academy of Sciences*, 112(2):354–359, 2015.

[23] Qibin Qi, Audrey Y Chu, Jae H Kang, Majken K Jensen, Gary C Curhan, Louis R Pasquale, Paul M Ridker, David J Hunter, Walter C Willett, Eric B Rimm, et al. Sugar-sweetened beverages and genetic risk of obesity. *New England Journal of Medicine*, 367(15):1387–1396, 2012.

bioRxiv preprint doi: https://doi.org/10.1101/2020.09.08.287888. this version posted September 9, 2020. The copyright holder for this preprint (which was not certified by peer review) is the author/funder. It is made available under a CC-BY 4.0 International license.

[24] Qibin Qi, Audrey Y Chu, Jae H Kang, Jinyan Huang, Lynda M Rose, Majken K Jensen, Liming Liang, Gary C Curhan, Louis R Pasquale, Janey L Wiggs, et al. Fried food consumption, genetic risk, and body mass index: gene-diet interaction analysis in three us cohort studies. *Bmj*, 348:g1610, 2014.

[25] Jiao Fang, Chun Gong, Yuhui Wan, Yuanyuan Xu, Fangbiao Tao, and Ying Sun. Polygenic risk, adherence to a healthy lifestyle, and childhood obesity. *Pediatric Obesity*, 14(4), 2019.

[26] K Komulainen, L Pulkki-Raback, M Jokela, LP Lyytikäinen, N Pitkänen, T Laitinen, M Hintsanen, M Elovainio, T Hintsa, A Jula, et al. Education as a moderator of genetic risk for higher body mass index: prospective cohort study from childhood to adulthood. *International Journal of Obesity*, 42(4):866–871, 2018.

[27] James Tabery. Biometric and developmental gene–environment interactions: Looking back, moving forward. *Development and Psychopathology*, 19(4):961–976, 2007.

[28] Arunabha Majumdar, Kathryn Burch, Sriram Sankararaman, Bogdan Pasaniuc, W James Gauderman, and John S Witte. A two-step approach to testing overall effect of gene-environment interaction for multiple phenotypes. *bioRxiv*, 2020.

[29] Lars Peter Hansen. Large sample properties of generalized method of moments estimators. *Econometrica: Journal of the Econometric Society*, pages 1029–1054, 1982.

[30] Daniel B Hall and Thomas A Severini. Extended generalized estimating equations for clustered data. *Journal of the American Statistical Association*, 93(444):1365–1375, 1998.

[31] Samuel A Lambert, Laurent Gil, Simon Jupp, Scott C Ritchie, Yu Xu, Annalisa Buniello, Gad Abraham, Michael Chapman, Helen Parkinson, John Danesh, et al. The polygenic score catalog: an open database for reproducibility and systematic evaluation. *medRxiv*, 2020.

[32] Jisu Shin and Sang Hong Lee. Gxesum: genotype-by-environment interaction model based on summary statistics. *BioRxiv*, 2020.

[33] Pierrick Wainschtein, Deepti P Jain, Loic Yengo, Zhili Zheng, L Adrienne Cupples, Aladdin H Shadyab, Barbara McKnight, Benjamin M Shoemaker, Braxton D Mitchell, Bruce M Psaty, et al. Recovery of trait heritability from whole genome sequence data. *BioRxiv*, page 588020, 2019.

[34] Elliot M Tucker-Drob. Measurement error correction of genome-wide polygenic scores in prediction samples. *bioRxiv*, page 165472, 2017.

[35] Felix C Tropf, S Hong Lee, Renske M Verweij, Gert Stulp, Peter J Van Der Most, Ronald De Vlaming, Andrew Bakshi, Daniel A Briley, Charles Rahal, Robert Hellpap, et al. Hidden heritability due to heterogeneity across seven populations. *Nature human behaviour*, 1(10):757–765, 2017.

[36] William H Greene. *Econometric Analysis*. McGraw-Hill. Inc. New York, fifth edition, 2002.

[37] O Komashko. nl waldtest: Wald test of nonlinear restrictions and nonlinear ci. *R package version*, 1(3), 2016.

[38] Ronald A Fisher. The correlation between relatives on the supposition of mendelian inheritance. *Earth and Environmental Science Transactions of the Royal Society of Edinburgh*, 52(2):399–433, 1919.

[39] Aysu Okbay, Jonathan P Beauchamp, Mark Alan Fontana, James J Lee, Tune H Pers, Cornelius A Rietveld, Patrick Turley, Guo-Bo Chen, Valur Emilsson, S Fleur W Meddens, et al. Genome-wide association study identifies 74 loci associated with educational attainment. *Nature*, 533(7604):539–542, 2016.

bioRxiv preprint doi: https://doi.org/10.1101/2020.09.08.287888. this version posted September 9, 2020. The copyright holder for this preprint (which was not certified by peer review) is the author/funder. It is made available under a CC-BY 4.0 International license.

[40] Delia Bugliari, Nancy Campbell, Chris Chan, Orla Hayden, Michael Hurd, Regan Main, Joshua Mallett, Colleen McCullough, Erik Meijer, Michael Moldoff, et al. Rand hrs data documentation, version p. *RAND Center for the Study of Aging*, 2016.

[41] Clare Bycroft, Colin Freeman, Desislava Petkova, Gavin Band, Lloyd T Elliott, Kevin Sharp, Allan Motyer, Damjan Vukcevic, Olivier Delaneau, Jared O'Connell, et al. The uk biobank resource with deep phenotyping and genomic data. *Nature*, 562(7726):203–209, 2018.

[42] Travis T Mallard, Richard K Linnér, Aysu Okbay, Andrew D Grotzinger, Ronald de Vlaming, S Fleur W Meddens, Elliot M Tucker-Drob, Kenneth S Kendler, Matthew C Keller, Philipp D Koellinger, and K. Paige Harden. Multivariate gwas of psychiatric disorders and their cardinal symptoms reveal two dimensions of cross-cutting genetic liabilities. *bioRxiv*, page 603134, 2020.

Acknowledements

The authors would like to thank Dan Benjamin, Dalton Conley, Michel Nivard, Paul Rathouz, Mijke Rhemtulla, and Patrick Turley for helpful comments on an early version of this manuscript. This research was conducted using the UK Biobank Resource (Application No. 36046). This work was supported in part by the National Science Foundation Graduate Research Fellowship Program under Grant No. DGE-1656518 (ST), by the Institute of Education Sciences under Grant No. R305B140009 (ST), by NIH grants R01MH120219, R01AG054628, and R01HD083613 (EMTD), and by the Jacobs Foundation (EMTD). Any opinions expressed are those of the authors alone and should not be construed as representing the opinions of funding agencies.

bioRxiv preprint doi: https://doi.org/10.1101/2020.09.08.287888. this version posted September 9, 2020. The copyright holder for this preprint (which was not certified by peer review) is the author/funder. It is made available under a CC-BY 4.0 International license.

Supplemental Information (SI)

A Methods

A.1 Description of the Heteroscedastic Regression Model and Derivation of ξ

The *environmental heteroscedasticity model* is specified as

$$Y_i = \tau_0 + \tau_1 E_i + \pi_0 G_i + \pi_1 G_i \cdot E_i + \lambda_0 \epsilon_i + \lambda_1 E_i \cdot \epsilon_i. \tag{9}$$

Here, τ_1 is the main effect of the measured environment, π_0 is the main effect of G_i, π_1 is the GxE directly analogous to β_3 in Eqn 1, λ_0 is the main effect of the error ϵ_i (which we assume, without loss of generality given λ_0, to have unit variance), and λ_1 is the coefficient used to index heteroscedasticity.

This model will produce very similar unstandardized estimates of GxE as the standard GxE model given by Eqn 1. In other words, π_1 in Eqn 9 is directly comparable to β_3 in Eqn 1. However, the heteroscedasticity model further models whether variance in the phenotype that is not accounted for by the genetic predictor (G_i) also varies as a function of the environment (E_i) in the form of an $E_i\epsilon_i$ interaction, as captured by the λ_1 parameter. Importantly, when G_i only index portions of total genetic etiology of a trait [33, 34, 35], the $E_i\epsilon_i$ interaction may result from GxE with respect to the genetic factors not indexed by Gi.

In order to test whether a more general pattern of heteroscedasticity as a function of E_i is sufficient to account for the observed GxE, we propose a restricted form version of this model that does not directly model GxE but instead allows for the total variance of the phenotype to vary as a function of E_i. This *scaling model* represents a scenario wherein GxE, in the sense of a significant estimate of β_3 in Eqn 1, arises as a function of differences in the total variance of Y as a function of E_i. The scaling model for moderation of the variance of Y_i as a function of E_i takes the form

$$Y_i = a_0 + a_1 E_i + (b_0 + b_1 E_i) Y_i^\star. \tag{10}$$

Here, E_i is a measured environment and $Y_i^\star$ is an unobserved factor representing unexplained variation in Y_i incremental of E_i. We introduce a scaling transformation that produces heteroscedasticity in Y_i as a function of E_i via the $b_0 + b_1 E_i$ coefficient on the $Y^\star$ term. We let

$$Y_i^\star = hG_i + e\epsilon_i \tag{11}$$

where G is a measured genotype standardized to have unit variance and ϵ_i is an unobserved error term (we assume it is also scaled to have unit variance). Finally, we set the scale of $Y^\star$ by specifying $e = \sqrt{1-h^2}$. The penetrance of the measured gentoype is thus controlled via the relative magnitudes of h and e. Note, in particular, that in terms of $Y_i^\star$, the penetrance of the measured genotype is constant. The test that we introduce relies on this property; i.e. that when properly scaled, the penetrance of the measured genotype to Y_i is constant in this model. Suppose that $b_1 = 0$. In that case, Y_i is affected solely by environmental and genetic main effects. If $b_1 \neq 0$, then the role of $Y_i^\star$ with respect to Y_i varies as a function of E, and as we elucidate next, so do the raw (but not relative) contributions of G_i and ϵ_i to Y.

Substituting Eqn 11 into Eqn 10, and setting $e = \sqrt{1-h^2}$, yields

$$\begin{aligned} Y_i &= a_0 + a_1 E_i + (b_0 + b_1 E_i)(hG_i + e\epsilon_i) && (12)\\ &= a_0 + a_1 E_i + b_0 hG_i + b_1 hE_i G_i + b_0 e\epsilon_i + b_1 eE_i\epsilon_i && (13)\\ &= a_0 + a_1 E_i + b_0 hG_i + b_1 hE_i G_i + b_0(\sqrt{1-h^2})\epsilon_i + b_1(\sqrt{1-h^2})E_i\epsilon_i && (14) \end{aligned}$$

It can be seen that the environmental scaling model (Eqn 14) constitutes a constrained form of the environmental heteroscedasticity model (Eqn 9). Both equations take the same form in terms

bioRxiv preprint doi: https://doi.org/10.1101/2020.09.08.287888. this version posted September 9, 2020. The copyright holder for this preprint (which was not certified by peer review) is the author/funder. It is made available under a CC-BY 4.0 International license.

of E and G. However, whereas the coefficients in Eqn 9 are unconstrained, these coefficients are linked to one another in Eqn 14 via the the ratio h/e which, as noted above, is fixed under the scaling model. Thus, Eqn 9 is equivalent to Eqn 14 when

$$\frac{\pi_0}{\lambda_0} = \frac{\pi_1}{\lambda_1}. \tag{15}$$

because, under Eqn 14

$$\frac{b_0 h}{b_0 e} = \frac{h}{e} = \frac{b_1 h}{b_1 e}. \tag{16}$$

i.e.

$$\frac{b_0 h}{b_0\sqrt{1-h^2}} = \frac{h}{\sqrt{1-h^2}} = \frac{b_1 h}{b_1\sqrt{1-h^2}}. \tag{17}$$

We use Eqn 15 as the basis for a hypothesis test. In particular, we consider the test statistic

$$\xi_E \equiv \widehat{\pi_0}\widehat{\lambda_1} - \widehat{\pi_1}\widehat{\lambda_0}, \tag{18}$$

$$H_0 : \xi_E = 0. \tag{19}$$

When $\xi_E = 0$, the environmental heteroscedasticity model is indistinguishable from the simpler scaling model, whereas when ξ_E is differs from 0, the environmental scaling model is rejected.

A.2 Estimation

We estimate Eqn 9 using maximum likelihood by assuming $\epsilon_i \sim \text{Normal}(0, 1)$.We assume that Y is mean-centered and that both G_i and E_i are non-random. Consider $\mathbb{E}(Y_i)$ and $\mathbb{V}(Y_i)$. We first have

$$\mathbb{E}(Y_i) = \tau_1 E_i + \pi_0 G_i + \pi_1 G_i \cdot E_i \tag{20}$$

since $\mathbb{E}(\epsilon) = 0$. We then have

$$\mathbb{V}(Y_i) = \mathbb{V}((\lambda_0 + \lambda_1 E_i)\epsilon) = (\lambda_0 + \lambda_1 E_i)^2 \tag{21}$$

since we assume $\mathbb{V}(\epsilon) = 1$. If we write

$$\theta = \{\tau_1, \pi_0, \pi_1, \lambda_0, \lambda_1\}, \tag{22}$$

note that both $\mathbb{E}(Y_i)$ and $\mathbb{V}(Y_i)$ are functions of θ.

Estimation of Eqn 9 is based on the likelihood,

$$L = \prod \phi\left(Y_i; \mathbb{E}(Y_i), \mathbb{V}(Y_i)\right) \tag{23}$$

where ϕ is the normal density and we use the above expressions for $\mathbb{E}(Y_i)$ and $\mathbb{V}(Y_i)$. We can thus solve for $\theta = \{\tau_1, \pi_0, \pi_1, \lambda_0, \lambda_1\}$ using ML based on

$$\log L = \sum \log \phi\left(Y_i; \mathbb{E}(Y_i), \mathbb{V}(Y_i)\right). \tag{24}$$

In particular, we obtain estimators via

$$\widehat{\theta_{\text{ML}}} = \text{argmax}_\theta \sum \log \phi\left(Y_i; \mathbb{E}(Y_i), \mathbb{V}(Y_i)\right). \tag{25}$$

To obtain ML estimates, it is convenient to also have the gradient. Here, we have

$$\frac{\partial \log L}{\tau_1} = \sum \frac{\partial \log L}{\partial \mu_i} E_i \tag{26}$$

$$\frac{\partial \log L}{\pi_0} = \sum \frac{\partial \log L}{\partial \mu_i} G_i \tag{27}$$

$$\frac{\partial \log L}{\pi_1} = \sum \frac{\partial \log L}{\partial \mu_i} G_i E_i \tag{28}$$

$$\frac{\partial \log L}{\lambda_0} = \sum \frac{\partial \log L}{\partial \sigma_i} \tag{29}$$

$$\frac{\partial \log L}{\lambda_1} = \sum \frac{\partial \log L}{\partial \sigma_i} E_i \tag{30}$$

bioRxiv preprint doi: https://doi.org/10.1101/2020.09.08.287888. this version posted September 9, 2020. The copyright holder for this preprint (which was not certified by peer review) is the author/funder. It is made available under a CC-BY 4.0 International license.

where $\mu_i = \mathbb{E}(Y_i)$, $\sigma_i = \sqrt{\mathbb{V}(Y_i)}$, and

$$\frac{\partial \log L}{\partial \mu_i} = \sum \frac{Y_i - \mu_i}{\sigma_i^2} \tag{31}$$

$$\frac{\partial \log L}{\partial \sigma_i} = (Y_i - \mu_i)^2 \sigma_i^{-3} - \sigma_i^{-1}. \tag{32}$$

Using these estimates, we can compute a test statistic. Replacing the values in Eqn 16 with estimates from Eqn 9, we propose to test

$$\frac{\widehat{\pi_0}}{\widehat{\lambda_0}} = \frac{\widehat{\pi_1}}{\widehat{\lambda_1}} \rightarrow \tag{33}$$

$$\xi_E \equiv \widehat{\pi_0}\widehat{\lambda_1} - \widehat{\pi_1}\widehat{\lambda_0}, \tag{34}$$

$$H_0 : \xi_E = 0. \tag{35}$$

If H_0 holds, the underlying form of GxE cannot be distinguished from the scaling phenomenon in which the total variance in Y_i varies as a function of E. Alternatively put, failure to reject H_0 constitutes a failure to reject the hypothesis that the *proportional* contributions of G_i and ϵ_i to Y_i do not vary with E.

H_0 can be tested via a Wald test for nonlinear restrictions. To test this nonlinear restriction, we consider (see Ref [36], Eqn 6-29)

$$W = \widehat{\xi_E} \cdot (\mathbb{V}(\xi_E))^{-1} \cdot \widehat{\xi_E}. \tag{36}$$

Given that we are testing a single restriction, W has a χ^2 distribution with one degree of freedom in large samples. To estimate $\mathbb{V}(\xi_E)$, we use the Hessian of Eqn 24 (see E) and the delta method. Computationally, we do this via [37]. Note also that conventional tests of π_1 and λ_1 can be used to offer insight into the existence of GxE and potential heteroscedasticity; we make use of such tests below.

A.3 Extensions

A version of the heteroscedasticity model presented in Eqn 9 above can be constructed so as to relax the assumption of homoscedasticity of residuals across G_i as follows

$$Y_i = \tau_0 + \tau_1 E_i + \pi_0 G_i + \pi_1 G_i \cdot E_i + \lambda_0 \epsilon_i + \lambda_2 G_i \cdot \epsilon_i. \tag{37}$$

Here λ_2 is the coefficient used to index heteroscedasticity as a function of G_i. We assume homoscedasticity of residuals as a function of E_i by omitting λ_1. We refer to Eqn 37 as a *genetic heteroscedasticity model*. When a single variant is entered for G, this model consitutes a vQTL model that includes a term for GxE. Note that this model is equivalent to the model presented in Eqn 9, but with G_i entered for E_i and E_i entered for G_i.

The scaling model for moderation of the variance of Y_i as a function of G_i takes the form

$$Y_i = d_0 + d_1 G_i + (f_0 + f_1 G_i) Y_i^\star. \tag{38}$$

and

$$Y_i^\star = sE_i + \sqrt{1 - s^2}\epsilon_i \tag{39}$$

As in the scaling model for moderation the variance of Y_i as a function of E_i, ϵ_i is assumed to have unit variance. In terms of $Y_i^\star$, the effect of E_i constant across G_i. However, in terms of Y_i, the effect of E_i changes across G_i as result of heteroscedasticity across G_i.

It follows that the hypothesis test comparing the GxE model allowing for heterocedasticity as a function of G_i (given by Eqn 37) to its reduced scaling model (given by Eqns 38 and 39, is

$$\xi_G \equiv \widehat{\tau_1}\widehat{\lambda_2} - \widehat{\pi_1}\widehat{\lambda_0}, \tag{40}$$

$$H_0 : \xi_G = 0. \tag{41}$$

bioRxiv preprint doi: https://doi.org/10.1101/2020.09.08.287888. this version posted September 9, 2020. The copyright holder for this preprint (which was not certified by peer review) is the author/funder. It is made available under a CC-BY 4.0 International license.

Finally, we can fit a *full heteroscedasticity model* that allows for moderation of residual variance in Y_i as a function of both G_i and E_i as follows

$$Y_i = \tau_0 + \tau_1 E_i + \pi_0 G_i + \pi_1 G_i \cdot E_i + \lambda_0 \epsilon_i + \lambda_1 E_i \cdot \epsilon_i + \lambda_2 G_i \cdot \epsilon_i. \tag{42}$$

This model may be particularly useful when there is nonzero gene-environment correlation between the two moderators, i.e. $\mid r(G_i, E_i) \mid > 0$, such that G_i and E_i can be mutually controlled when modelling heteroscedasticity. However, to avoid added complexity, we recommend that comparisons with the scaling models rely on the ξ_E and ξ_G tests from the separate environmental heteroscedasticity and genetic heteroscedasticity models, respectively.

bioRxiv preprint doi: https://doi.org/10.1101/2020.09.08.287888. this version posted September 9, 2020. The copyright holder for this preprint (which was not certified by peer review) is the author/funder. It is made available under a CC-BY 4.0 International license.

B Simulation Study

We now consider both the null distribution of the test statistic under different configurations of the relevant parameters from the scaling model (Eqn 14) and the performance of our test statistic in the case of generating models that do not conform to the scaling model (i.e. when Eqn 1 is used to generate a model with GxE and homoscedastic residuals, or Eqn 9 is used to general a model with heteroscedastic residuals but no GxE). We primarily describe the simulation models in the context of the heteroscadasticity and scaling models in which the measured environment, E_i moderates the residual variance of the phenotype, Y_i, as given by Eqns 9 and 14. However, as described in A.3, these models are equivalent to those in which the measured phenotype, G_i moderates the residual variance of Y_i (after G_i and E_i are substituted for one another). Thus simulation results apply to both scenarios.

B.1 Distribution of the test statistic under H_0

We first consider the behavior of the test statistic when the null hypothesis is true. We generate data according to the *scaling model* (Eqn 14), estimate the *heteroscedasticity model* (Eqn 9), and then calculate the ξ_E test statistic and associated Wald-based probability. We start by illustrating that the appropriate transformation of ξ_E has a χ^2 distribution. To do this, we generate 10,000 datasets from the scaling model (Eqn 14) with $b_0 = 1, b_1 = 0.15, h = 0.5, N = 5000$. We compute ξ_E and then transform it to W via Eqn 36. Results are in Figure B.1. The null distribution of W neatly aligns with the density of $\chi^2(1)$. Below, we report on ξ_E given that it is a relatively intuitive function of the estimated parameters but also exploit the fact that ξ_E can be mapped to W and inference can be done via reference to $\chi^2(1)$.

Figure B.1: Comparison of distribution of W under the null hypothesis to $\chi^2(1)$.

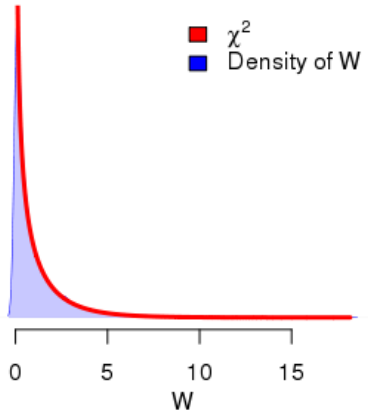

We next considered the behavior of ξ_E under the null, for configurations of the relevant parameters in the scaling model (Eqn 14) meant to capture the relevant features of an analysis in which G is a PGS. We considered variation in four parameters. We used three different sample sizes (1000, 5000, 10000). We used two values respectively for b_0 (0.8, 1) and b_1 (0.05, 0.1). Finally, we used two values for h (0.1 and 0.5). The values of h suggest weakly (0.1) to strongly (0.5) penetrant genetic predictors; they were chosen to represent the range of potential PGS predictors given existing technology [33]. Recall that the value of e is fixed as a function of h. Note that we considered two different distributions for E; we sampled E from both the standard normal and the uniform distributions (where the uniform distribution was scaled to have the same standard deviation as the standard normal). As polygenic scores for complex traits are expected to be normally distributed [38], G was sampled from the standard normal distribution. To help develop intuition, suppose $b_0 = 0.8$, $b_1 = 0.05$, and $h = 0.5$. In that case, $\mathbb{V}(y|E = 2) = 0.736$ compared to $\mathbb{V}(y|E = -2) = 0.422$, a ratio of 1.74 (i.e., there is heteroscedasticity). Finally, it is important to note that the scale of ξ_E is dependent on several features (e.g. scale of G and E); patterns shown

bioRxiv preprint doi: https://doi.org/10.1101/2020.09.08.287888. this version posted September 9, 2020. The copyright holder for this preprint (which was not certified by peer review) is the author/funder. It is made available under a CC-BY 4.0 International license.

here are informative about the behavior of ξ_E but the values themselves do not necessarily generalize to other cases (e.g., if E or G does not have unit variance). In contrast, W and associated tests are invariant to scaling of G and E, but sensitive to sample size.

Results are shown in Table B.1. Note that the estimates of ξ_E are unbiased (i.e., the means are nearly zero). Further, as we would anticipate, the false positive rate (FPR) of the test is insensitive to the parameters; note also that the mean probability associated with the test of ξ_E via Eqn 36 is near 0.05, as we would expect when the null is true.[2]

In contrast, the variance of the test statistic (and, thus, statistical power) depends on the sample size and simulation parameters. In particular, note the decline in the SD of the test statistics as a function of the sample size. Statistical power will also depend upon h; this test will have less power with less penetrant genetic predictors.

Table B.1: Distribution of ξ_E under the null (mean and SD) and associated test (Eqn 36) for different values of parameters in Eqn 14. For each set of parameters, 1000 datasets are simulated. Normal and Uniform refer to the distributions used to generate the environmental variable.

Simulation Parameters				Results (Normal E_i)				Results (Uniform E_i)			
N	b_0	b_1	h	Mean(ξ_E)	SD(ξ_E)	Mean(Pr_{ξ_E})	FPR(ξ_E)	Mean(ξ_E)	SD(ξ_E)	Mean(Pr_{ξ_E})	FPR(ξ_E)
1000	0.80	0.05	0.10	1.58e-04	0.02	0.50	0.06	-9.05e-04	0.01	0.51	0.04
1000	1.00	0.05	0.10	3.71e-04	0.03	0.50	0.06	1.11e-03	0.02	0.50	0.05
1000	0.80	0.10	0.10	-5.53e-05	0.02	0.49	0.06	3.63e-04	0.01	0.50	0.05
1000	1.00	0.10	0.10	3.66e-04	0.03	0.49	0.05	-7.39e-04	0.02	0.50	0.05
1000	0.80	0.05	0.50	3.46e-04	0.02	0.49	0.05	-6.60e-05	0.01	0.49	0.05
1000	1.00	0.05	0.50	1.30e-03	0.02	0.51	0.04	-1.98e-04	0.02	0.50	0.04
1000	0.80	0.10	0.50	3.35e-04	0.02	0.50	0.05	7.74e-04	0.01	0.50	0.04
1000	1.00	0.10	0.50	-6.83e-04	0.03	0.51	0.05	-6.09e-05	0.02	0.50	0.05
5000	0.80	0.05	0.10	1.31e-04	0.01	0.51	0.05	-2.31e-04	0.01	0.52	0.04
5000	1.00	0.05	0.10	1.78e-04	0.01	0.52	0.04	-1.95e-04	0.01	0.49	0.05
5000	0.80	0.10	0.10	-2.32e-04	0.01	0.49	0.05	4.81e-06	0.01	0.51	0.04
5000	1.00	0.10	0.10	1.83e-04	0.01	0.49	0.05	5.02e-04	0.01	0.51	0.04
5000	0.80	0.05	0.50	1.59e-04	0.01	0.51	0.06	-1.48e-04	0.01	0.50	0.05
5000	1.00	0.05	0.50	-8.10e-05	0.01	0.47	0.05	2.47e-04	0.01	0.50	0.05
5000	0.80	0.10	0.50	1.95e-04	0.01	0.49	0.06	-8.94e-05	0.00	0.50	0.05
5000	1.00	0.10	0.50	4.67e-04	0.01	0.49	0.05	3.49e-05	0.01	0.51	0.05
10000	0.80	0.05	0.10	1.29e-04	0.01	0.50	0.04	-2.16e-05	0.00	0.49	0.07
10000	1.00	0.05	0.10	-9.81e-05	0.01	0.50	0.04	6.69e-05	0.01	0.50	0.05
10000	0.80	0.10	0.10	1.89e-04	0.01	0.49	0.04	1.85e-04	0.00	0.51	0.05
10000	1.00	0.10	0.10	-9.32e-05	0.01	0.50	0.05	4.98e-05	0.01	0.52	0.04
10000	0.80	0.05	0.50	2.62e-04	0.01	0.50	0.05	-4.27e-05	0.00	0.51	0.05
10000	1.00	0.05	0.50	2.56e-05	0.01	0.49	0.05	-1.42e-04	0.01	0.50	0.04
10000	0.80	0.10	0.50	-2.30e-04	0.00	0.49	0.06	-1.89e-04	0.00	0.51	0.04
10000	1.00	0.10	0.50	-3.71e-04	0.01	0.49	0.06	-6.03e-05	0.01	0.49	0.05

We next considered the behavior of of ξ_E under the null for configurations of parameters meant to capture the relevant features of an analysis in which G is an allele count for a single locus (e.g. a SNP). Results are in Table B.2. The table is similar to Table B.1, but where we now consider allele counts based on variants simulated under a binomial distribution with different minor allele frequencies (denoted p). Based on Extended Data Figure 2 in [39], we chose effect sizes of $h^2 \in \{.05\%, .1\%\}$. Note that after generating G under a binomial distribution, it was standardized, such that h can be interpreted as a standardized effect size. We examine behavior using a sample size of $N = 10000$, which might be used for confirmatory tests of a select number of variants previously identified in a larger independent GWAS, and a sample size of $N = 1000000$, which might be used for genome-wide discovery. Simulation results indicate that the heteroscedasticity model and the ξ_E statistic behave as expected across the range of conditions examined.

[2]We use Pr_β to refer to probability associated with a test of the null hypothesis that some parameter β equals zero.

bioRxiv preprint doi: https://doi.org/10.1101/2020.09.08.287888. this version posted September 9, 2020. The copyright holder for this preprint (which was not certified by peer review) is the author/funder. It is made available under a CC-BY 4.0 International license.

Table B.2: Distribution of ξ_E under the null (mean and SD) and associated test (via Eqn 36) for different values of parameters in Eqn 14 based on a standardized single-locus allele count. For each set of parameters, 100 datasets are simulated. The environmental variable is sampled from the standard normal distribution.

N	b_0	b_1	h	MAF	$\widehat{\pi_1}$	$\widehat{\lambda_1}$	Mean(ξ_E)	SD(ξ_E)	Mean(Pr$_{\xi_E}$)	$\frac{\mathbb{E}(SE(\xi_E))}{SD(\xi_E)}$
10000	0.80	0.05	0.02	0.01	6.91e-04	0.05	3.25e-04	6.50e-03	0.51	0.97
10000	1.00	0.05	0.02	0.01	6.52e-04	0.05	4.67e-04	9.76e-03	0.49	1.02
10000	0.80	0.10	0.02	0.01	3.25e-03	0.10	-7.18e-04	6.35e-03	0.47	0.95
10000	1.00	0.10	0.02	0.01	2.53e-03	0.10	-3.72e-04	9.29e-03	0.52	1.05
10000	0.80	0.05	0.03	0.01	1.17e-03	0.05	3.92e-04	6.18e-03	0.52	1.02
10000	1.00	0.05	0.03	0.01	1.81e-03	0.05	-1.64e-04	1.13e-02	0.47	0.88
10000	0.80	0.10	0.03	0.01	2.29e-03	0.10	8.04e-04	6.13e-03	0.48	0.98
10000	1.00	0.10	0.03	0.01	2.43e-03	0.10	7.48e-04	9.56e-03	0.49	1.01
100000	0.80	0.05	0.02	0.01	1.27e-03	0.05	-1.12e-04	1.96e-03	0.52	1.02
100000	1.00	0.05	0.02	0.01	6.32e-04	0.05	4.75e-04	3.10e-03	0.47	1.01
100000	0.80	0.10	0.02	0.01	2.00e-03	0.10	1.59e-04	1.84e-03	0.52	1.03
100000	1.00	0.10	0.02	0.01	2.49e-03	0.10	-2.23e-04	2.97e-03	0.50	1.02
100000	0.80	0.05	0.03	0.01	1.21e-03	0.05	2.92e-04	2.11e-03	0.47	0.94
100000	1.00	0.05	0.03	0.01	1.40e-03	0.05	1.70e-04	2.88e-03	0.52	1.09
100000	0.80	0.10	0.03	0.01	3.04e-03	0.10	7.05e-05	2.16e-03	0.46	0.88
100000	1.00	0.10	0.03	0.01	2.53e-03	0.10	5.93e-04	3.04e-03	0.53	1.00
10000	0.80	0.05	0.02	0.05	3.28e-03	0.05	-1.73e-03	5.97e-03	0.52	1.06
10000	1.00	0.05	0.02	0.05	1.03e-03	0.05	9.44e-05	1.15e-02	0.41	0.86
10000	0.80	0.10	0.02	0.05	2.20e-03	0.10	1.36e-04	5.53e-03	0.53	1.08
10000	1.00	0.10	0.02	0.05	2.61e-03	0.10	-8.78e-06	1.04e-02	0.47	0.93
10000	0.80	0.05	0.03	0.05	7.91e-04	0.05	6.14e-04	6.44e-03	0.47	0.98
10000	1.00	0.05	0.03	0.05	1.51e-03	0.05	-4.78e-06	1.13e-02	0.47	0.88
10000	0.80	0.10	0.03	0.05	4.31e-03	0.10	-7.83e-04	6.14e-03	0.50	0.98
10000	1.00	0.10	0.03	0.05	4.16e-03	0.10	-9.08e-04	9.64e-03	0.48	0.99
100000	0.80	0.05	0.02	0.05	1.16e-03	0.05	-5.90e-05	1.98e-03	0.54	1.00
100000	1.00	0.05	0.02	0.05	7.56e-04	0.05	3.44e-04	3.06e-03	0.49	1.02
100000	0.80	0.10	0.02	0.05	1.74e-03	0.10	3.91e-04	2.03e-03	0.48	0.93
100000	1.00	0.10	0.02	0.05	2.20e-03	0.10	3.24e-05	3.20e-03	0.47	0.95
100000	0.80	0.05	0.03	0.05	1.72e-03	0.05	-9.93e-05	1.83e-03	0.54	1.09
100000	1.00	0.05	0.03	0.05	1.31e-03	0.05	2.68e-04	3.31e-03	0.46	0.95
100000	0.80	0.10	0.03	0.05	3.69e-03	0.10	-3.60e-04	2.15e-03	0.44	0.88
100000	1.00	0.10	0.03	0.05	3.09e-03	0.10	5.50e-05	3.35e-03	0.45	0.91
10000	0.80	0.05	0.02	0.50	-4.27e-04	0.05	1.22e-03	6.81e-03	0.48	0.92
10000	1.00	0.05	0.02	0.50	1.53e-03	0.05	-4.68e-04	8.87e-03	0.53	1.11
10000	0.80	0.10	0.02	0.50	1.60e-03	0.10	5.75e-04	6.84e-03	0.45	0.87
10000	1.00	0.10	0.02	0.50	3.90e-03	0.10	-1.55e-03	9.61e-03	0.53	0.99
10000	0.80	0.05	0.03	0.50	1.35e-03	0.05	1.87e-04	6.44e-03	0.51	0.98
10000	1.00	0.05	0.03	0.50	3.36e-03	0.05	-1.68e-03	9.08e-03	0.56	1.08
10000	0.80	0.10	0.03	0.50	4.00e-03	0.10	-6.84e-04	5.63e-03	0.52	1.06
10000	1.00	0.10	0.03	0.50	3.78e-03	0.10	-5.68e-04	9.75e-03	0.50	0.99
100000	0.80	0.05	0.02	0.50	1.34e-03	0.05	-1.60e-04	2.00e-03	0.48	1.00
100000	1.00	0.05	0.02	0.50	7.07e-04	0.05	4.14e-04	2.91e-03	0.51	1.08
100000	0.80	0.10	0.02	0.50	2.21e-03	0.10	3.19e-05	1.92e-03	0.51	0.99
100000	1.00	0.10	0.02	0.50	2.00e-03	0.10	2.02e-04	2.73e-03	0.55	1.11
100000	0.80	0.05	0.03	0.50	1.89e-03	0.05	-2.42e-04	2.24e-03	0.44	0.89
100000	1.00	0.05	0.03	0.50	1.99e-03	0.05	-4.30e-04	3.26e-03	0.52	0.96
100000	0.80	0.10	0.03	0.50	3.00e-03	0.10	1.23e-04	2.04e-03	0.44	0.92
100000	1.00	0.10	0.03	0.50	3.51e-03	0.10	-3.25e-04	2.96e-03	0.50	1.02

bioRxiv preprint doi: https://doi.org/10.1101/2020.09.08.287888. this version posted September 9, 2020. The copyright holder for this preprint (which was not certified by peer review) is the author/funder. It is made available under a CC-BY 4.0 International license.

B.2 Performance under alternatives

We now turn to study the behavior of the heteroscedasticity model and associated ξ_E test statistic when the null hypothesis is false (i.e., when Eqn 14 is not the data generating model). We consider two different data generating models: (i) a model with GxE and homoscedastic residuals, generated according to Eqn 1 (ii) a model with no GxE but with heteroscedastic residuals, generated according to Eqn 9. In these analyses, we aim to probe whether the test statistic allows us to reject H_0 under different configurations of the relevant data-generating parameters.

We first study a circumstance in which the generating model is GxE with homoscedastic residuals. We use Eqn 1 for our data-generating model and suppose that e_i is white-noise (i.e., $e_i \sim \mathrm{N}(0, \sigma^2)$) as opposed to heteroscedastic as a function of E_i. In particular, we set $\sigma^2 = 1$. We focus on two tests: a test of whether $\pi_1 = 0$ and a test of whether $\xi_E = 0$. Data are analyzed with the environmental heteroscadasticity model (Eqn 9, which subsumes Eqn 1).

Results are shown in Table B.3. When both N and b_3 are relatively small, we are poorly powered to detect GxE and to reject the scaling hypothesis (i.e., both Pr_{π_1} and Pr_{ξ_E} are relatively large). Importantly, when GxE is not detected, the ξ_E test is moot. In contrast, power to detect GxE and to reject scaling are both excellent when N or b_3 is relatively large. Throughout we reject $\lambda_1 = 0$ for $\alpha = .05$ at the appropriate FPR.

Table B.3: Behavior of ξ_E when true model is homoscedastic GxE (Eqn 1). Behavior is shown for 1000 simulated datasets based on each set of parameters.

Simulation Parameters				Results				
N	β_1	β_2	β_3	Mean(Pr_{π_1})	Power(π_1)	Mean(Pr_{ξ_E})	Power(ξ_E)	FPR(λ_1)
1000	0.10	0.00	0.05	2.45e-01	3.48e-01	2.48e-01	3.48e-01	0.05
1000	0.20	0.00	0.05	2.26e-01	3.33e-01	2.31e-01	3.35e-01	0.05
1000	0.10	0.20	0.05	2.36e-01	3.56e-01	2.38e-01	3.57e-01	0.07
1000	0.20	0.20	0.05	2.16e-01	3.87e-01	2.21e-01	3.80e-01	0.05
1000	0.10	0.50	0.05	2.40e-01	3.34e-01	2.41e-01	3.32e-01	0.05
1000	0.20	0.50	0.05	2.23e-01	3.57e-01	2.26e-01	3.41e-01	0.06
1000	0.10	0.00	0.15	7.68e-04	9.98e-01	8.40e-04	9.97e-01	0.05
1000	0.20	0.00	0.15	9.08e-04	9.97e-01	1.01e-03	9.95e-01	0.04
1000	0.10	0.20	0.15	8.63e-04	9.98e-01	8.68e-04	9.97e-01	0.06
1000	0.20	0.20	0.15	6.13e-04	9.97e-01	6.72e-04	9.98e-01	0.05
1000	0.10	0.50	0.15	8.49e-04	9.96e-01	9.04e-04	9.97e-01	0.06
1000	0.20	0.50	0.15	9.02e-04	9.97e-01	1.14e-03	9.95e-01	0.06
5000	0.10	0.00	0.05	1.30e-02	9.37e-01	1.30e-02	9.32e-01	0.04
5000	0.20	0.00	0.05	9.69e-03	9.53e-01	1.03e-02	9.47e-01	0.06
5000	0.10	0.20	0.05	1.39e-02	9.37e-01	1.39e-02	9.32e-01	0.05
5000	0.20	0.20	0.05	1.26e-02	9.34e-01	1.34e-02	9.30e-01	0.05
5000	0.10	0.50	0.05	1.29e-02	9.43e-01	1.29e-02	9.43e-01	0.04
5000	0.20	0.50	0.05	1.52e-02	9.36e-01	1.60e-02	9.36e-01	0.05
5000	0.10	0.00	0.15	3.05e-13	1.00e+00	1.36e-12	1.00e+00	0.06
5000	0.20	0.00	0.15	1.62e-17	1.00e+00	9.32e-17	1.00e+00	0.04
5000	0.10	0.20	0.15	1.58e-15	1.00e+00	1.16e-15	1.00e+00	0.05
5000	0.20	0.20	0.15	2.74e-17	1.00e+00	5.83e-17	1.00e+00	0.04
5000	0.10	0.50	0.15	7.99e-18	1.00e+00	2.30e-17	1.00e+00	0.05
5000	0.20	0.50	0.15	1.48e-14	1.00e+00	2.87e-14	1.00e+00	0.05

We next consider the circumstance in which there is no GxE, but there are G and E main effects, and there is heteroscedasticity as a function of E so as to parallel Eqn 21. In particular, we generate data via

$$Y_i = b_1 G_i + b_2 E_i + \epsilon_i \tag{43}$$

with $\epsilon_i \sim \mathrm{N}(0, (\lambda_0 + \lambda_1 E_i)^2)$. We use $\lambda_0 = 2$ and vary λ_1 between 0.15 and 0.3 (if $\lambda_1 = 0$, there is no heteroscedasticity). We focus on tests of $\pi_1 = 0, \lambda_1 = 0, \xi_E = 0$.

Results are shown in Table B.4. First, note that the appropriate FPR of .05 is obtained for $\pi_1 = 0$ at alpha=.05, irrespective of λ_0 and λ_1. This indicates that heteroscedasticity has not induced the impression of GxE under these conditions. We can also uniformly detect that $\lambda_1 \neq 0$ suggesting that errors are in fact heteroscedastic. However, tests of ξ_E are relatively weak here

bioRxiv preprint doi: https://doi.org/10.1101/2020.09.08.287888. this version posted September 9, 2020. The copyright holder for this preprint (which was not certified by peer review) is the author/funder. It is made available under a CC-BY 4.0 International license.

(e.g., power is 0.2 at best). Importantly, as the tests of π_1 appropriate indicate no GxE, the question of whether there is scaling GxE is moot.

Table B.4: Behavior of ξ_E when true model does not have GxE but does have heteroscedastic error (Eqn 43). Behavior is shown for 1000 simulated datasets based on each set of parameters.

Simulation Parameters					Results					
N	π_0	τ_1	λ_0	λ_1	Mean($\Pr_{\pi_1}$)	FPR(π_1)	Mean($\Pr_{\lambda_1}$)	Power(λ_1)	Mean($\Pr_{\xi_E}$)	Power(ξ_E)
1000.00	0.10	0.00	2.00	0.15	0.50	0.06	2.03e-02	0.90	0.49	0.05
1000.00	0.20	0.00	2.00	0.15	0.50	0.05	1.55e-02	0.93	0.49	0.06
1000.00	0.10	0.50	2.00	0.15	0.49	0.07	1.74e-02	0.92	0.48	0.07
1000.00	0.20	0.50	2.00	0.15	0.50	0.05	1.70e-02	0.93	0.48	0.06
1000.00	0.10	0.00	2.00	0.30	0.50	0.05	1.62e-06	1.00	0.48	0.05
1000.00	0.20	0.00	2.00	0.30	0.50	0.05	8.32e-07	1.00	0.45	0.09
1000.00	0.10	0.50	2.00	0.30	0.50	0.06	5.46e-06	1.00	0.49	0.07
1000.00	0.20	0.50	2.00	0.30	0.49	0.05	8.40e-07	1.00	0.46	0.07
5000.00	0.10	0.00	2.00	0.15	0.51	0.06	1.25e-08	1.00	0.51	0.06
5000.00	0.20	0.00	2.00	0.15	0.49	0.05	9.85e-08	1.00	0.46	0.09
5000.00	0.10	0.50	2.00	0.15	0.49	0.06	6.29e-09	1.00	0.48	0.06
5000.00	0.20	0.50	2.00	0.15	0.50	0.05	5.07e-08	1.00	0.46	0.08
5000.00	0.10	0.00	2.00	0.30	0.49	0.06	6.79e-36	1.00	0.45	0.10
5000.00	0.20	0.00	2.00	0.30	0.50	0.06	1.95e-37	1.00	0.33	0.22
5000.00	0.10	0.50	2.00	0.30	0.49	0.05	7.32e-38	1.00	0.44	0.09
5000.00	0.20	0.50	2.00	0.30	0.49	0.06	1.48e-38	1.00	0.32	0.23

bioRxiv preprint doi: https://doi.org/10.1101/2020.09.08.287888. this version posted September 9, 2020. The copyright holder for this preprint (which was not certified by peer review) is the author/funder. It is made available under a CC-BY 4.0 International license.

C Software

Code to estimate the heteroscestacity model and to estimate ξ_E is available in an R package.[3] In particular, the documentation illustrates functionality via simple simulations similar to those found in Section B.

[3] `https://github.com/ben-domingue/scalingGxE`

bioRxiv preprint doi: https://doi.org/10.1101/2020.09.08.287888. this version posted September 9, 2020. The copyright holder for this preprint (which was not certified by peer review) is the author/funder. It is made available under a CC-BY 4.0 International license.

D Data

D.1 HRS Data

The first wave of HRS data collection was in 1992, the most recent in 2018 (wave 13). We focus on N=11,586 respondents of European ancestry. Descriptive information for the environment and outcome are shown in Figure D.1. We use data from the RAND HRS files on BMI, see [40] for additional documentation. In particular, we consider the mean BMI over all waves. The mean BMI was skewed, so we also considered a transformed version (see Figure D.1). HRS respondents were born across a wide span of birthyears centered around 1940. To ensure that results aren't driven by small numbers of observations with extreme birth years, we analyzed those born between 1920–1965. All data (polygenic score, birthyear, and BMI) are standardized to have mean zero and unit variance for analysis.

Figure D.1: Top: Density of BMI and birthyear in HRS data as well as QQ plot of the Box-Cox transformed version (meant to reduce skew). We standardize respondent's average BMI taken over all waves; this mean BMI is skewed (skew equals 1.14). This is a common finding with respect to BMI (see, for example, the Figure in [14]). Thus, we also consider a version of this variable in which it has been transformed, via the Box-Cox transformation, to closely approximate a normal distribution. All variables (birthyear, polygenic score, and outcome) are standardized (to have zero mean and unit variance) prior to analysis. Bottom: Illustration of increasing variance in BMI distribution as a function of birth year for analytic sample.

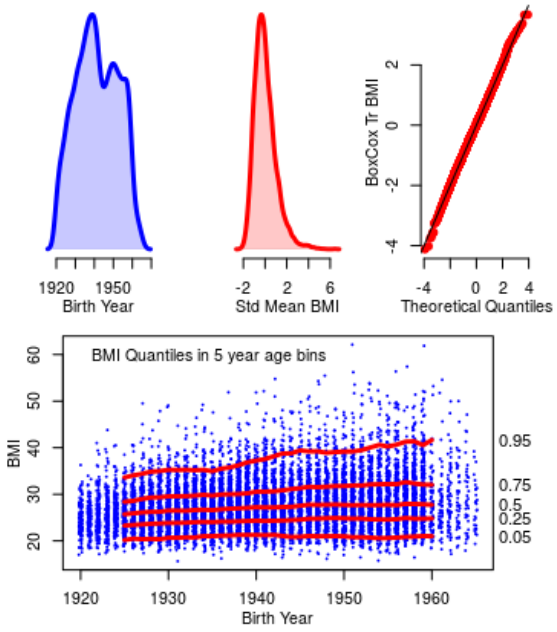

D.2 UKB data

We used data from UK Biobank to conduct a series of SNP-level gene-by-environment association analyses. Genotyping and imputation procedures were performed by the original UK Biobank investigators, as described in a previous publication [41].[4] In the present study, we applied additional thresholds to minimize potential confounding, removing participants with (i) low call rate, (ii) extreme heterozygosity, (iii) chromosomal aneuploidy, (iv) discordant self-reported and chromosomal sex, or (v) missing data for the relevant outcome and covariates. We further focused our

[4]See also `https://www.ukbiobank.ac.uk/scientists-3/genetic-data/`.

bioRxiv preprint doi: https://doi.org/10.1101/2020.09.08.287888. this version posted September 9, 2020. The copyright holder for this preprint (which was not certified by peer review) is the author/funder. It is made available under a CC-BY 4.0 International license.

analyses on unrelated participants of non-Hispanic European ancestry to minimize the threat of population stratification.

Rather than perform a genome-wide scan of gene-by-environment interactions, we focused on our analyses on loci that have been previously associated with BMI. Specifically, we selected the 97 loci identified in a large genome-wide association study of body mass index that did not include UK Biobank [16]. We successfully identified and extracted the lead SNP for 96/97 (99%) of these loci. For imputed SNPs, dosages were converted to hard calls. Any converted hard calls with a certainty less than .90 were coded as missing.

As some UK Biobank participants had multiple observations for BMI, we computed the mean BMI for each individual. We applied a Box-Cox transformation to reduce skew. Box-Cox transformed BMI was then adjusted for sex, batch, and the first 40 principal components of ancestry, which we estimated ourselves [42]. All variables (SNP, birth year, and body mass index) were standardized to have mean zero and unit variance prior to analysis. The final analytic samples size was N=380,605.

bioRxiv preprint doi: https://doi.org/10.1101/2020.09.08.287888. this version posted September 9, 2020. The copyright holder for this preprint (which was not certified by peer review) is the author/funder. It is made available under a CC-BY 4.0 International license.

E The Hessian

We use the Hessian ($\frac{\partial^2 \log L}{\partial \theta^2}$) for construction of the covariance matrix of the estimation errors for the model parameters under the null model. The constituent parts of the Hessian are as follows.

$$\frac{\partial^2 \log L}{\partial \tau_1^2} = \sum_i -E_i^2 \sigma_i^{-2} \tag{44}$$

$$\frac{\partial^2 \log L}{\partial \tau_1 \partial \pi_0} = \sum_i -E_i G_i \sigma_i^{-2} \tag{45}$$

$$\frac{\partial^2 \log L}{\partial \tau_1 \partial \pi_1} = \sum_i -E_i^2 G_i \sigma_i^{-2} \tag{46}$$

$$\frac{\partial^2 \log L}{\partial \tau_1 \partial \lambda_0} = \sum_i -2E_i (Y_i - \mu_i) \sigma_i^{-3} \tag{47}$$

$$\frac{\partial^2 \log L}{\partial \tau_1 \partial \lambda_1} = \sum_i -2E_i^2 (Y_i - \mu_i) \sigma_i^{-3} \tag{48}$$

$$\frac{\partial^2 \log L}{\partial \pi_0^2} = \sum_i -G_i^2 \sigma_i^{-2} \tag{49}$$

$$\frac{\partial^2 \log L}{\partial \pi_0 \partial \pi_1} = \sum_i -E_i G_i^2 \sigma_i^{-2} \tag{50}$$

$$\frac{\partial^2 \log L}{\partial \pi_0 \partial \lambda_0} = \sum_i -2G_i (Y_i - \mu_i) \sigma_i^{-3} \tag{51}$$

$$\frac{\partial^2 \log L}{\partial \pi_0 \partial \lambda_1} = \sum_i -2E_i G_i (Y_i - \mu_i) \sigma_i^{-3} \tag{52}$$

$$\frac{\partial^2 \log L}{\partial \pi_1^2} = \sum_i -E_i^2 G_i^2 \sigma_i^{-2} \tag{53}$$

$$\frac{\partial^2 \log L}{\partial \pi_1 \partial \lambda_0} = \sum_i -2E_i G_i (Y_i - \mu_i) \sigma_i^{-3} \tag{54}$$

$$\frac{\partial^2 \log L}{\partial \pi_1 \partial \lambda_1} = \sum_i -2E_i^2 G_i (Y_i - \mu_i) \sigma_i^{-3} \tag{55}$$

$$\frac{\partial^2 \log L}{\partial \lambda_0^2} = \sum_i \left[\sigma_i^{-2} - 3(Y_i - \mu_i)^2 \sigma_i^{-4} \right] \tag{56}$$

$$\frac{\partial^2 \log L}{\partial \lambda_0 \partial \lambda_1} = \sum_i \left[E_i \sigma_i^{-2} - 3E_i (Y_i - \mu_i)^2 \sigma_i^{-4} \right] \tag{57}$$

$$\frac{\partial^2 \log L}{\partial \lambda_1^2} = \sum_i \left[E_i^2 \sigma_i^{-2} - 3E_i^2 (Y_i - \mu_i)^2 \sigma_i^{-4} \right] \tag{58}$$

$$\tag{59}$$

bioRxiv preprint doi: https://doi.org/10.1101/2020.09.08.287888. this version posted September 9, 2020. The copyright holder for this preprint (which was not certified by peer review) is the author/funder. It is made available under a CC-BY 4.0 International license.

F Supplemental Tables

Table F.1: vQTL discoveries for BMI. From the 96 marker SNPs for genome-wide significant loci for BMI in [16], those reaching significance at $p < .05/96$ for moderation of variance, as indicated by the λ_2 coefficient from the full heterscedasticity model. Parameters are reported for the full heteroscedasticity model, with ξ_E and ξ_G parameters from the environmental and genetic heteroscedasticity models, respectively

SNP	π_0	π_1	$\Pr_{\pi_1}$	λ_0	λ_1	λ_2	$\Pr_{\lambda_2}$	$\Pr_{\xi_E}$	$\Pr_{\xi_G}$
rs2207139_A	-0.02	-0.00	3.76e-03	0.99	0.04	-0.00	8.93e-05	1.39e-02	3.84e-03
rs7903146_C	0.01	-0.00	6.48e-01	0.99	0.04	0.01	3.22e-06	8.09e-01	9.02e-01
rs9925964_A	0.02	-0.00	9.07e-01	0.99	0.04	0.00	1.10e-04	6.11e-01	7.50e-01
rs1558902_T	-0.05	-0.01	2.12e-06	0.99	0.04	-0.01	1.76e-17	2.96e-04	5.14e-07
rs6567160_T	-0.03	-0.00	1.65e-02	0.99	0.04	-0.01	2.84e-08	8.97e-02	1.40e-02
rs2287019_C	0.02	-0.00	8.71e-01	0.99	0.04	0.01	8.15e-06	8.27e-01	6.66e-01

bioRxiv preprint doi: https://doi.org/10.1101/2020.09.08.287888. this version posted September 9, 2020. The copyright holder for this preprint (which was not certified by peer review) is the author/funder. It is made available under a CC-BY 4.0 International license.

Table F.2: Replication of main effects at $p < .05/96$ for the 96 marker SNPs for the genome-wide significant loci for BMI in [16]. Main effects (π_0) come from the full heteroscedasity model.

SNP	π_0	SE(π_0)	$\Pr_{\pi_0}$	Replication?
rs977747_G	-0.0119	0.0016	1.3380e-13	TRUE
rs657452_G	-0.0116	0.0016	6.3858e-13	TRUE
rs11583200_T	-0.0103	0.0016	1.8037e-10	TRUE
rs3101336_C	0.0152	0.0016	1.8616e-21	TRUE
rs12566985_A	-0.0133	0.0016	1.3812e-16	TRUE
rs12401738_G	-0.0103	0.0016	1.4297e-10	TRUE
rs11165643_T	0.0125	0.0016	6.5757e-15	TRUE
rs17024393_T	-0.0146	0.0016	1.8806e-19	TRUE
rs543874_A	-0.0271	0.0016	2.2391e-63	TRUE
rs2820292_C	0.0131	0.0016	2.6984e-16	TRUE
rs13021737_G	0.0279	0.0016	1.6738e-68	TRUE
rs10182181_A	-0.0243	0.0016	2.0290e-51	TRUE
rs11126666_G	-0.0021	0.0016	1.9697e-01	FALSE
rs1016287_C	-0.0128	0.0016	1.4586e-15	TRUE
rs11688816_G	0.0083	0.0016	3.0389e-07	TRUE
rs2121279_C	-0.0050	0.0016	2.0019e-03	FALSE
rs1460676_T	-0.0083	0.0016	2.7992e-07	TRUE
rs1528435_T	0.0101	0.0016	2.8226e-10	TRUE
rs17203016_A	-0.0071	0.0016	1.0494e-05	TRUE
rs7599312_G	0.0116	0.0016	9.6039e-13	TRUE
rs492400_T	-0.0072	0.0016	7.8542e-06	TRUE
rs2176040_G	-0.0014	0.0016	3.7490e-01	FALSE
rs6804842_G	0.0088	0.0016	5.6154e-08	TRUE
rs2365389_C	0.0092	0.0016	1.0286e-08	TRUE
rs3849570_C	-0.0075	0.0016	2.5934e-06	TRUE
rs13078960_T	-0.0109	0.0016	1.3418e-11	TRUE
rs16851483_G	-0.0124	0.0016	1.3755e-14	TRUE
rs1516725_C	0.0162	0.0016	4.0089e-24	TRUE
rs10938397_A	-0.0208	0.0016	1.5818e-38	TRUE
rs17001654_C	-0.0069	0.0016	2.3970e-05	TRUE
rs13107325_C	-0.0187	0.0016	2.1694e-31	TRUE
rs11727676_T	0.0014	0.0016	3.9716e-01	FALSE
rs2112347_T	0.0189	0.0016	5.4850e-32	TRUE
rs7715256_T	-0.0106	0.0016	3.8649e-11	TRUE
rs205262_A	-0.0185	0.0016	8.4528e-31	TRUE
rs2033529_A	-0.0132	0.0016	2.5074e-16	TRUE
rs2207139_A	-0.0209	0.0016	3.0425e-38	TRUE
rs9400239_C	0.0098	0.0016	1.0575e-09	TRUE
rs9374842_T	0.0059	0.0016	2.1120e-04	TRUE
rs13201877_A	-0.0048	0.0016	2.8052e-03	FALSE
rs13191362_A	0.0086	0.0016	8.0189e-08	TRUE
rs1167827_G	0.0155	0.0016	4.3736e-22	TRUE
rs2245368_T	-0.0133	0.0016	2.0238e-16	TRUE
rs9641123_G	-0.0052	0.0016	1.1563e-03	FALSE
rs6465468_G	-0.0032	0.0016	4.6521e-02	FALSE

bioRxiv preprint doi: https://doi.org/10.1101/2020.09.08.287888. this version posted September 9, 2020. The copyright holder for this preprint (which was not certified by peer review) is the author/funder. It is made available under a CC-BY 4.0 International license.

SNP	π_0	SE(π_0)	$\Pr_{\pi_0}$	Replication?
rs17405819_T	0.0137	0.0016	1.2564e-17	TRUE
rs16907751_C	0.0074	0.0016	4.3644e-06	TRUE
rs2033732_C	0.0065	0.0016	4.8454e-05	TRUE
rs4740619_T	0.0140	0.0016	2.4629e-18	TRUE
rs10968576_A	-0.0149	0.0016	1.5486e-20	TRUE
rs6477694_T	-0.0088	0.0016	4.7682e-08	TRUE
rs1928295_T	0.0083	0.0016	1.9969e-07	TRUE
rs10733682_G	-0.0101	0.0017	1.0969e-09	TRUE
rs7899106_A	-0.0086	0.0016	1.0639e-07	TRUE
rs17094222_T	-0.0070	0.0016	1.2704e-05	TRUE
rs11191560_T	-0.0085	0.0016	1.2063e-07	TRUE
rs7903146_C	0.0094	0.0016	4.1177e-09	TRUE
rs4256980_G	0.0113	0.0016	1.8886e-12	TRUE
rs11030104_A	0.0219	0.0016	1.6990e-42	TRUE
rs2176598_C	-0.0136	0.0016	1.9700e-17	TRUE
rs3817334_C	-0.0179	0.0016	6.0633e-29	TRUE
rs12286929_G	0.0113	0.0016	2.4293e-12	TRUE
rs7138803_G	-0.0179	0.0016	1.0766e-28	TRUE
rs11057405_G	0.0122	0.0016	2.3471e-14	TRUE
rs12429545_G	-0.0125	0.0016	1.3652e-14	TRUE
rs9540493_G	-0.0085	0.0016	1.2686e-07	TRUE
rs1441264_A	0.0126	0.0017	4.0919e-14	TRUE
rs10132280_C	0.0143	0.0016	1.3063e-18	TRUE
rs12885454_C	0.0110	0.0016	5.7772e-12	TRUE
rs11847697_C	-0.0072	0.0016	7.7682e-06	TRUE
rs7141420_T	0.0145	0.0016	5.3645e-19	TRUE
rs3736485_G	-0.0082	0.0016	3.5057e-07	TRUE
rs16951275_T	0.0159	0.0016	3.9682e-23	TRUE
rs7164727_T	0.0104	0.0016	9.0124e-11	TRUE
rs758747_C	-0.0088	0.0016	7.5808e-08	TRUE
rs12446632_G	0.0149	0.0016	2.1385e-20	TRUE
rs2650492_G	-0.0124	0.0016	1.7199e-14	TRUE
rs3888190_C	-0.0191	0.0016	1.1586e-32	TRUE
rs4787491_G	0.0126	0.0016	4.9604e-15	TRUE
rs9925964_A	0.0165	0.0016	1.0272e-24	TRUE
rs2080454_A	-0.0057	0.0016	4.8633e-04	TRUE
rs1558902_T	-0.0503	0.0016	1.0423e-214	TRUE
rs9914578_C	-0.0064	0.0016	6.7263e-05	TRUE
rs1000940_A	-0.0105	0.0016	5.9037e-11	TRUE
rs12940622_G	0.0129	0.0016	1.1756e-15	TRUE
rs1808579_C	0.0131	0.0016	3.3014e-16	TRUE
rs7239883_A	-0.0073	0.0016	6.8097e-06	TRUE
rs7243357_T	0.0092	0.0016	9.8026e-09	TRUE
rs6567160_T	-0.0311	0.0016	5.0802e-83	TRUE
rs17724992_A	0.0111	0.0016	5.1966e-12	TRUE
rs29941_G	0.0093	0.0016	7.1063e-09	TRUE
rs2075650_A	0.0113	0.0016	1.7586e-12	TRUE
rs2287019_C	0.0183	0.0016	4.9748e-30	TRUE
rs3810291_A	0.0191	0.0016	8.5285e-33	TRUE
rs6091540_C	0.0134	0.0016	1.1496e-16	TRUE
rs2836754_C	0.0076	0.0016	1.8681e-06	TRUE